Runoff and mass balance of the Greenland ice sheet: 1958–2003

Edward Hanna,[1] Philippe Huybrechts,[2,3] Ives Janssens,[3] John Cappelen,[4] Konrad Steffen,[5] and Ag Stephens[6]

Received 29 November 2004; revised 9 March 2005; accepted 11 April 2005; published 12 July 2005.

[1] Meteorological models were used to retrieve annual accumulation, runoff, and surface mass balance on a 5 km × 5 km grid for the Greenland ice sheet for 1958–2003. We present the first such history that provides insight into seasonal and interannual variability, which should prove useful for those studying the ice sheet. Derived runoff was validated by means of a control model run and independent in situ data. Modeled accumulation has already been validated using shallow ice core data. Surface mass balance (SMB) responds rapidly on a yearly basis to changing meteorological (surface air temperature and precipitation) forcing. There are distinct signals in runoff and SMB following three major volcanic eruptions. Runoff losses from the ice sheet were 264 (±26) km^3 yr^{-1} in 1961–1990 and 372 (±37) km^3 yr^{-1} in 1998–2003. Significantly rising runoff since the 1990s has been partly offset by increased precipitation. Our best estimate of overall mass balance declined from 22 (±51) km^3 yr^{-1} in 1961–1990 to −36 (±59) km^3 yr^{-1} in 1998–2003, which is not statistically significant. Additional dynamical factors that cause an acceleration of ice flow near the margins, and possible enhanced iceberg calving, may have led to a more negative mass balance in the past few years than suggested here. The implication is a significant and accelerating recent contribution from the ice sheet to global sea level rise, with 0.15 mm yr^{-1} from declining SMB alone over the last 6 years.

Citation: Hanna, E., P. Huybrechts, I. Janssens, J. Cappelen, K. Steffen, and A. Stephens (2005), Runoff and mass balance of the Greenland ice sheet: 1958–2003, *J. Geophys. Res.*, *110*, D13108, doi:10.1029/2004JD005641.

1. Introduction

[2] The Greenland ice sheet (GrIS) is the world's second largest ice mass and is potentially highly vulnerable to ongoing climatic variability and change, in particular anthropogenic global warming, because its margins are already relatively warm compared with, say, Antarctica, with summer mean air temperatures around 3–9°C [*Cappelen et al.*, 2001]. Indeed a rise of >3 K in Greenland annual average temperature (which seems likely to be achieved by 2100) accompanying anthropogenic climate change is likely to cause an irreversible melting of the GrIS unless radical greenhouse gas emission reductions are made within the next few decades [*Gregory et al.*, 2004]. Surface meltwater runoff already accounts for approximately 57 (±9)% of the ice sheet's current annual mass loss, the total annual mass loss approximately equaling the mass gained from snow accumulation [*Church et al.*, 2001]. Modeling studies have shown that for every 1 K rise in surface air temperature, 20–50% more Greenland ice melt is produced [*Oerlemans*, 1991; *Braithwaite and Olesen*, 1993; *Ohmura et al.*, 1996; *Janssens and Huybrechts*, 2000], with satellite data showing a concomitant 47% K^{-1} increase in GrIS snowmelt extent [*Abdalati and Steffen*, 2001], so summer temperature rises of only ~2–5 K are required to double melt rates and thereby substantially increase runoff and hence mass lost from the ice sheet. Recent observational studies suggest the likelihood of accelerated ice flow, and presumed enhanced iceberg calving, in a warmer climate [*Krabill et al.*, 2004; *Zwally et al.*, 2002].

[3] Given its importance in the global climate/change arena, it is therefore disconcerting that we still do not even know the sign of mass balance of the GrIS, although recent airborne laser surveys suggest an overall negative balance, with an estimated 0.13 mm yr^{-1} mean contribution to global sea level rise during 1993–1998 increasing to 0.20 mm yr^{-1} during 1997–2003 [*Krabill et al.*, 2004]. The question remains how representative is this kind of short-term (few years') measurement of longer-term (multidecadal) state of balance and change?

[4] In order to improve predictions of future behavior of the GrIS it is necessary to better assess its current state and variability. Models are useful in this respect, because of paucity of data with time and space, especially when they are validated using appropriate observations. Modeled snow accumulation based on European Centre for Medium-Range

[1]Department of Geography, University of Sheffield, Sheffield, UK.
[2]Alfred Wegener Institute, Bremerhaven, Germany.
[3]Departement Geografie, Vrije Universiteit, Brussels, Belgium.
[4]Danish Meteorological Institute, Copenhagen, Denmark.
[5]Cooperative Institute for Research in Environmental Sciences, University of Colorado, Boulder, Colorado, USA.
[6]British Atmospheric Data Centre, Rutherford Appleton Laboratory, Chilton, UK.

0148-0227/05/2004JD005641$09.00

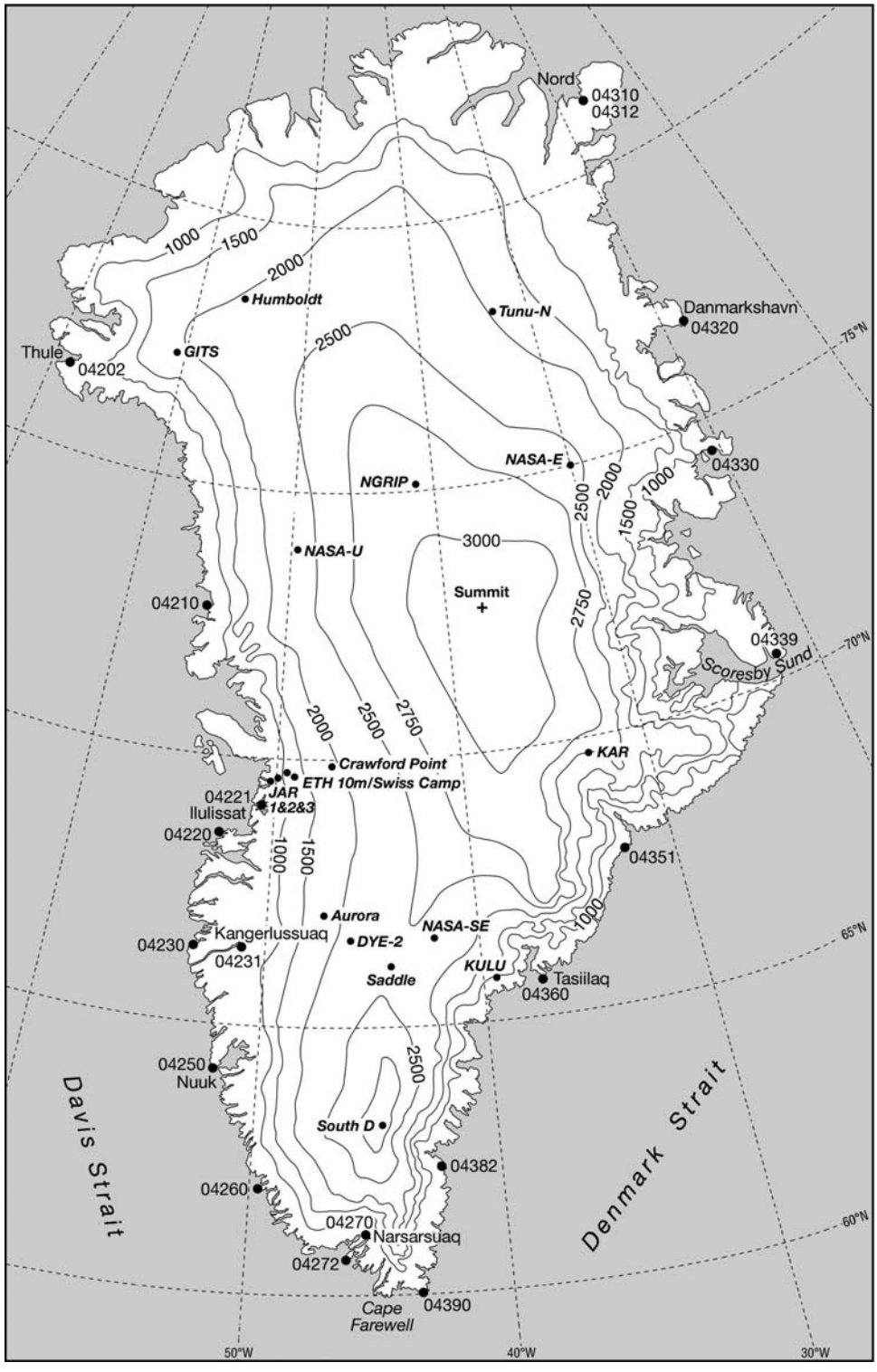

Figure 1. Greenland station location map, also showing elevation contours.

Weather Forecasts (ECMWF) reanalyzed snowfall and surface latent heat flux/evaporation has been compared with shallow ice core data and shown to perform well overall for Greenland [*Hanna et al.*, 2001, 2005]. There is significant interannual and spatial variability in Greenland precipitation minus evaporation and snow accumulation, but no long-term trend is clearly apparent. We need to quantify runoff, the principal mass output, as well as accumulation, the main mass input, to help constrain current GrIS surface mass balance (SMB = snow accumulation minus runoff).

[5] *Braithwaite et al.* [1992] constructed 6–8 year runoff series for different periods for the 1970s/1980s from three sites at the GrIS margin and, relating these to summer mean temperature and precipitation data from nearby Danish

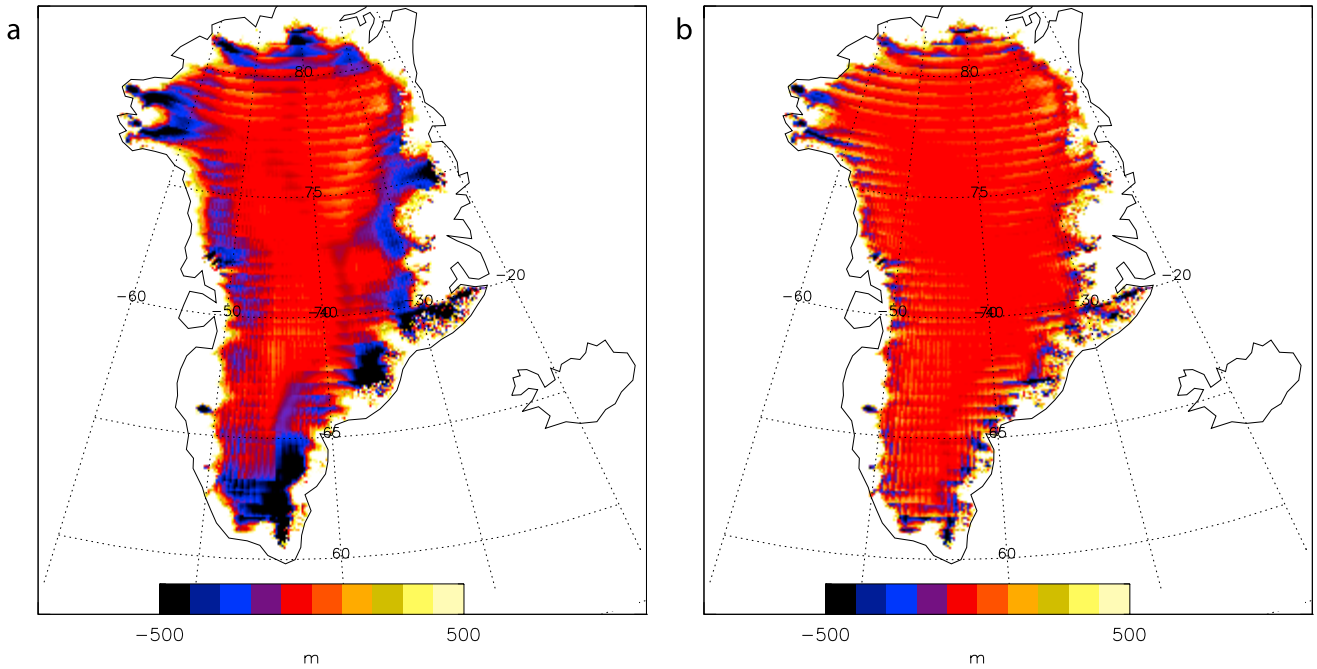

Figure 2. (a) ERA-40 orography minus Huybrechts/Ekholm orography. (b) ECMWF 2002 orography minus Huybrechts/Ekholm orography.

Meteorological Institute weather stations, constructed runoff series for each site for 30 years (1961–1990). They found substantial and apparently random interannual variations of ±0.5 m yr^{-1} water in net ablation (runoff) but high correlations between the runoff series, which are reasonably spread across southwest Greenland. *Braithwaite et al.* [1992] found no overall trend for the 30-year period, but they noted relatively high runoff in the early 1960s followed by relatively low runoff from the late 1960s until the mid-1980s. However, there is a requirement to extrapolate upward from these pioneering field measurements to the ice sheet scale. *Mote* [2003] used passive microwave satellite brightness temperature data and a positive degree day model to model GrIS runoff and SMB on a 25-km grid for 1988–1999. He derived an average runoff of 278 km^3 yr^{-1} and SMB of 261 km^3 yr^{-1} for the whole ice sheet. *Box et al.* [2004] used the Polar MM5 mesoscale climate model on a 24-km grid and in situ automatic weather station (AWS) data to derive GrIS mass balance for 1991–2000. They suggest a large interannual variability (= 10-year range of annual values) of ±187 km^3 yr^{-1} for total ice sheet SMB, which is equivalent to the magnitude of the SMB. Consideration of far more years of runoff and SMB than both these studies is needed in order to reliably find and define any significant climatically forced trend that may be present in the glaciological interannual mass balance series.

[6] In this paper we derive and discuss 1958–2003 GrIS runoff and SMB data based on (re)analysis data from the ECMWF and an annual/monthly degree-day surface meltwater runoff/retention model. We explain our modeling techniques and both background driving and validation data for the models in sections 2 and 3. Runoff is derived in section 4, and our definitive GrIS SMB series is presented in section 5; the latter section also includes preliminary considerations of runoff and SMB links with climate. In section 6 we discuss implications for overall GrIS mass balance and global sea level rise. Concluding remarks are made in section 7. Greenland locations referred to in our study are shown in Figure 1.

2. Background Data and Downscaling Method

2.1. ECMWF Data and Downscaling

[7] Six-hourly surface air temperature (SAT) and 12- and 36-hour forecast total (large-scale plus convective) precipitation (P) and surface latent heat flux (SLHF) for 1958–2003 were obtained from the ECMWF. These data were bilinearly interpolated from a nominal resolution of 1.125° latitude × 1.125° longitude to a 0.5° × 0.5° grid. They were based on ERA-40 reanalysis data for 1958–2001 and later ECMWF operational analyses for 2002 and 2003. The reanalysis consists of a global climatological time series of model-consistent data generated by a numerical weather prediction model run retrospectively, feeding in all available observations to a 3D-Var data assimilation system [*Simmons and Gibson*, 2000]. Operational analyses are derived from updated forms of the ECMWF model run in real time. Latent heats of vaporization and sublimation were used to calculate evaporation (for SAT > 0°C) and sublimation (for SAT ≤ 0°C) (E) from the SLHF data. All fields were averaged monthly and then resampled/downscaled to a ~5 km × 5 km polar stereographic grid, the minimum resolution considered necessary to accurately model runoff, which occurs and intensifies in a very narrow zone around the GrIS margins [*Janssens and Huybrechts*, 2000]. This is not just a resampling: SAT, on which modeled melt most depends, was empirically corrected during the downscaling process (section 2.4). P and E were downscaled using straightforward (fuzzy) interpolation which involved finding the weighted ($1/d^2$) average of the values of four

Table 1. Height Differences (Hdiff) and Surface Air Temperature Differences (Tdiff) Between (Raw) ECMWF Model and Surface Stations[a]

Station	Hdiff, m	Tdiff_year, K	Tdiff_summer, K
DMI 04202	457	−4.5	−2.6
04210	256	−1.5	−1.4
04220	254	−2.2	1.0
04221	480	−5.5	−4.9
04230	228	−1.0	2.2
04231	593	−1.9	−3.8
04250	364	−1.7	−2.4
04260	868	−5.4	−4.1
04270	665	−7.1	−8.6
04272	156	−1.0	−2.7
04310	157	−0.9	−1.6
04320	138	−1.3	−1.2
04330	518	−2.8	−2.7
04339	11	−1.0	−1.3
04351	962	−4.5	−1.9
04360	180	−0.8	−2.6
04382	533	−0.8	−1.6
04390	85	1.2	−0.6
DMI mean	383.6	−2.4	−2.3
GC-Net Swiss Camp	−224	1.6	1.2
Crawford Point 1	−178	3.7	3.0
NASA-U	−83	3.1	3.1
GITS	−511	5.5	5.6
Humboldt	−122	4.1	4.1
Summit	−120	2.2	3.9
Tunu-N	−37	3.7	4.6
DYE-2	−153	4.2	3.5
JAR 1	−18	−0.2	0.2
Saddle	−186	3.4	3.1
South Dome	−552	3.4	4.6
NASA-E	−225	4.4	6.0
Crawford Point 2	−185	3.5	2.6
NGRIP	−98	2.5	3.7
NASA-SE	−16	−0.6	0.6
KAR	−314	3.0	4.4
JAR2	322	−2.0	−1.2
JAR3	274	−2.6	−1.7
GC-Net mean	−134.8	2.4	2.9

[a]Tdiff is given for the year and summer (JJA) season. Positive bias means ECMWF relatively higher value.

ECMWF pixels nearest to each successive pixel of the finer-resolution grid.

[8] The relatively coarse (T159 ≅ 110 km) resolution of the ECMWF model used to produce the ERA-40 reanalysis results in extensive spectral rippling over Greenland through the Gibbs effect and resulting surface elevations that are often several hundred meters in error over the GrIS, even though the ECMWF model itself incorporates (P. Viterbo, personal communication, 2002) the relatively accurate (<10s m) Ekholm orography [*Ekholm*, 1996] (Figure 2a). ERA-40 thus has biases of typically 2–3 K in SAT when compared with in situ meteorological station data (Table 1). This is obviously unacceptable if realistic runoff modeling is to be attempted because of the great sensitivity of modeled runoff to SAT (see section 1). The situation is considerably improved in later (2002 and 2003) ECMWF operational analyses because the model used to produce these had a much higher horizontal resolution (T511 ≅ 40 km). However, some considerable, several hundred meter local biases in surface elevation still exist (Figure 2b). We adjust SAT to allow for these orography errors (section 2.4). Linear features along lines of latitude in Figure 2 are artefacts of resampling from the relatively coarse ECMWF grid to the finer-resolution polar stereographic grid.

2.2. In Situ Validation Data

[9] We use in situ data to validate our meteorological model. For most of the period these are from synoptic weather stations of the Danish Meteorological Institute (DMI) [*Cappelen et al.*, 2001]: We identify those used in this study by their five-digit World Meteorological Organization (WMO) codes on Figure 1. DMI station monthly SAT data are based on temperature measurements taken every 3 hours according to standard WMO guidelines whereby a thermometer is placed inside a radiation shield 2 m above ground. The homogeneity of the DMI SAT time series has been examined using all available metadata and is considered not to have been significantly affected by site relocation or redevelopments [*Cappelen et al.*, 2001].

[10] For the last few years we make use of badly needed stations inland in the form of the Greenland Climate Network (GC-Net) [*Steffen and Box*, 2001]. GC-Net currently consists of 21 automatic weather stations (AWSs) with a distributed coverage over the Greenland ice sheet (Figure 1). Four stations are located along the crest of the ice sheet (2500–3200 m elevation range) in a north-south direction, ten stations are located close to the 2000-m contour line (1830–2500 m), and seven stations were positioned in the ablation region (560–1150 m).

[11] The GC-Net was initiated in spring 1995 with the intention of monitoring climatological and glaciological parameters at various locations on the ice sheet over a time period of at least 15 years [*Steffen and Box*, 2001]. The first AWS was installed in 1991 at the Swiss Camp with objectives to measure daily, annual, and interannual variability in accumulation rate, surface climatology, and surface energy balance. At each AWS a total of 32 climate parameters are sampled every 15 s and averaged over an hour and then transmitted via a satellite link: GOES for station locations south of 72°N and Argos for the stations north of 72°N. GC-Net instruments are factory-calibrated; nonetheless, on-site relative calibrations are performed at most annual site visits to ensure good quality of the data. For air temperature, type E thermocouples are used, mounted in radiation shields which are not actively ventilated but "naturally aspirated" due to the constant katabatic wind along the slope of the ice sheet. Some overheating is possible in areas of low wind speed and high solar radiation, like on top of the ice sheet. The thermocouples have a relative accuracy of 0.1°C and an absolute accuracy of approximately 0.3°C.

2.3. Ice Sheet Surface Lapse Rates

[12] Empirically derived "lapse rates" (i.e., at the ice sheet surface, not equivalent with the free atmospheric lapse rate) were calculated on the basis of plotting ECMWF model in situ station mean SAT differences (annual and seasonal) against ECMWF model in situ station height differences, the latter from Figure 2, using the ERA-40 geopotential (orography) and 1957–2001 SAT data. Eighteen DMI synoptic surface meteorological stations (low lying and mainly around the coast) and 18 GC-Net AWSs (the latter higher up and inland with many greater than ~2000-m elevation, see above discussion) were used in the

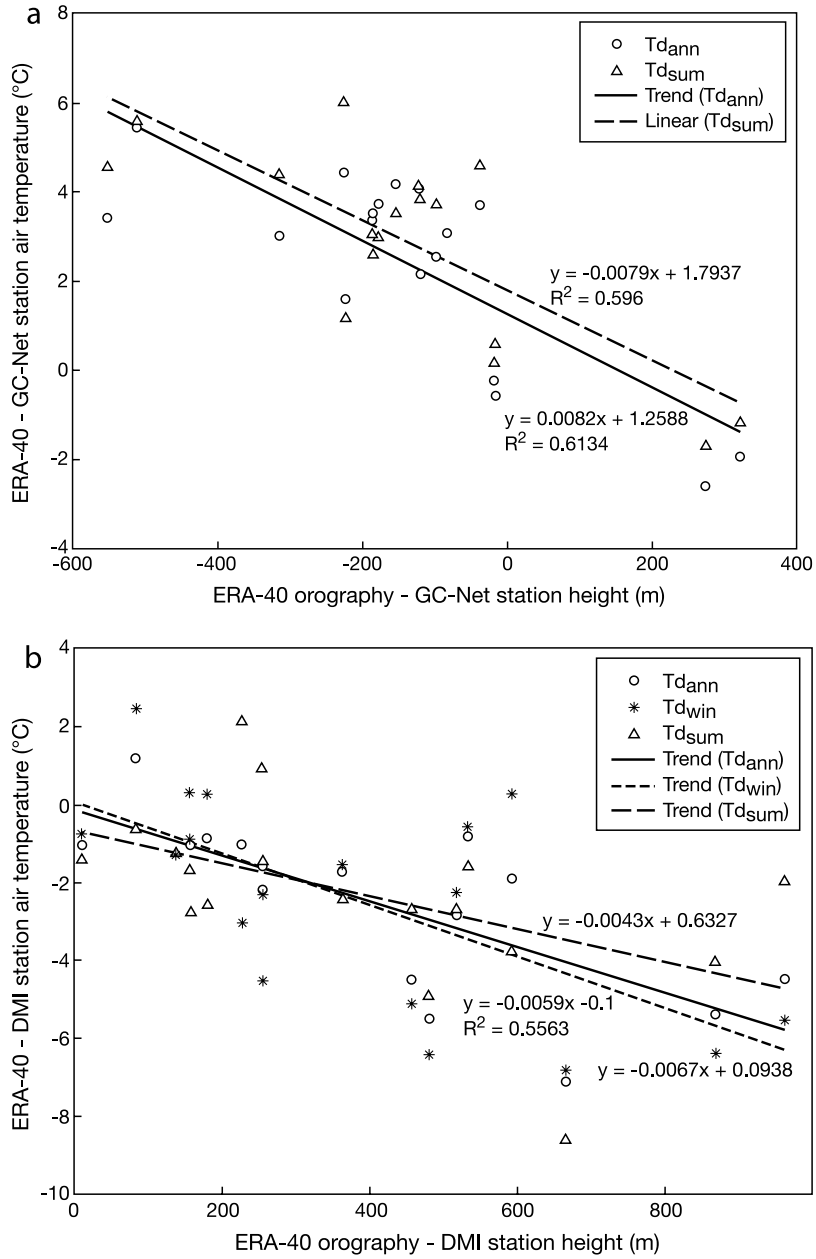

Figure 3. (a) ERA-40 minus GC-Net station surface air temperature differences versus ERA-40 minus GC-Net station height differences. (b) ERA-40 minus DMI station surface air temperature differences versus ERA-40 minus DMI station height differences.

intercomparisons (Table 1). Together these give a good distribution of stations across the GrIS (Figure 1). Resulting regression line slopes yielded annual (summer = JJA) "lapse rates" of −8.2 (−7.9) K km^{-1} for the bulk of the GrIS >1000 m elevation (Figure 3a) and −5.9 (−4.3) K km^{-1} for low-lying marginal regions ≤1000 m (Figure 3b). The latter rates are probably shallower owing to SAT inversions experienced around the GrIS margins. The observed relationships between SAT and height differences are statistically significant at the $p < 0.05$ level. This relationship was also seen in the case of earlier ECMWF reanalysis (ERA-15) SAT data [*Hanna and Valdes*, 2001]. Our empirically derived lapse rates give generally similar results to the *Huybrechts and de Wolde* [1999] sinusoidal surface temperature parameterization: The latter gives −8.0 K km^{-1} mean annual LR but zero LR below a latitude-dependent inversion height of up to 300 m and −6.3 K km^{-1} LR in July). However, our lapse rates suggest a weaker seasonal cycle that is almost absent above 1000 m.

[13] The near-surface temperature lapse rate is important for the parameterization of climatic variables on the ice sheet. The AWS mean monthly air temperatures along the western slope of the ice sheet, from Summit (3200 m), Crawford Point (CP, 2020 m), and Swiss Camp (1170 m) were normalized to 70°N using a latitudinal temperature gradient of −0.78 K/1° latitude [*Steffen and Box*, 2001].

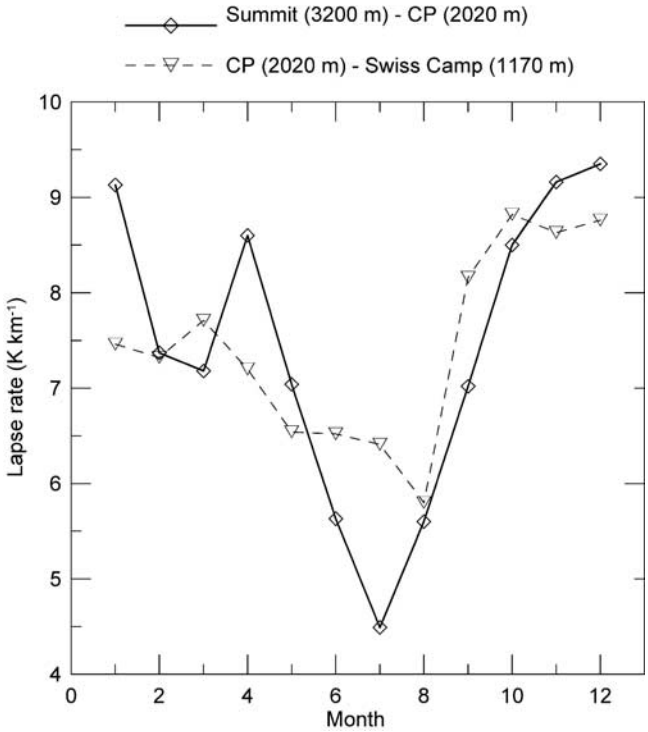

Figure 4. Multiyear monthly mean lapse rate along the western slope of the Greenland ice sheet as derived from AWS data normalized to 70°N with latitudinal gradient of −0.78°C/1° latitude for the profile Summit to Crawford Point (CP) and CP to Swiss Camp. The multiyear (1995–2003) annual mean lapse rates for both height profiles are 7.4 K km^{-1}.

This analysis reveals a mean annual lapse rate (1995–2003) of −7.4 K km^{-1} for both height profiles, Summit to CP and CP to Swiss Camp, respectively (Figure 4), much in agreement with our comparison of modeled with in situ heights and temperatures. The surface lapse rate along the western slope of the ice sheet at 70°N varies considerably during one annual cycle with values approaching the saturated adiabatic lapse rate (∼10 K km^{-1} in cold air) in winter but as low as 4.5 K km^{-1} in summer. This is not revealed during our model versus in situ analysis, possibly because the model already accounts to some extent for seasonal variations. The monthly lapse rate for the profile Swiss Camp to JAR1 (960 m) and JAR2 (542 m), which means below 1000 m elevation, is very similar to the one shown for CP to Swiss Camp.

2.4. Model Surface Air Temperature Corrections

[14] In the present study we "corrected" SAT during the downscaling process at ∼5 × 5-km resolution on the basis of our derived surface lapse rates and differences between the ECMWF orography schemes and a definitive Greenland DEM adapted from *Ekholm* [1996] with some small corrections made to surface elevation of ice shelves (Figure 2). Our corrected modeled SAT is within 0.02 (−0.10) K of the DMI station observed annual (summer) SATs averaged across the DMI station locations, and within 1 K at 10/18 of the DMI station locations, although larger scatter exists for a few individual DMI station locations (SAT model bias −3.1 K at 04270 and +2.3 K at 04382) (Table 2). Nevertheless, we feel that this is an impressive result that brings modeled SAT into close alignment with observed SAT. There is a greater discrepancy (annual mean +1.28 K, rising to +1.65 K in summer) with GC-Net AWS SATs. There seems to be a spatial pattern in the surface air temperature difference between corrected ECMWF and GC-Net in situ measurements. The largest differences of 2.9 to 3.1 K are found in the north for Humboldt and Tunu-N stations with model data too warm. Given the cold temperatures in the north of Greenland, we hypothesize that the true lapse rate is larger, as has been noted during winter months along the west slope of Greenland (Figure 4). All the comparative locations on top of the ice sheet like Summit, GITS, and NGRIP have also a model warm bias around 1.5 K, and the same arguments applies here as for the northern stations. It is interesting that all the locations along the west slope around 2000 m elevation (CP1, NASA-U, DYE-2, CP2, and Aurora) also have model warm anomalies around 2 K, which are hard to explain on the basis of lapse rates. On the other hand, stations in the east and southeast of Greenland show a cold anomaly in the corrected ECMWF data (S-Dome, NASA-SE, and KULU). These regions are known for the warm and moist air advection from the Atlantic by the frequent Icelandic cyclones. In summary, remaining deficiencies in either orographic forcing or the boundary layer scheme in the ECMWF model [see *Hanna et al.*, 2001] might be responsible for the remaining slight warm model bias over the upper reaches of the ice sheet. However, most of this area lies well above the zone of significant runoff, and modeled SATs are in much better agreement with observed for the lower-lying (<1750 m) GC-Net stations (Swiss Camp, JAR1, JAR2, KULU, and JAR3): mean modeled-observed SAT difference = 0.01 (0.79) K for the year (summer) for these stations. This elevation range encompasses most of the runoff zone [*Janssens and Huybrechts*, 2000]. Overall, our corrected model temperatures for the runoff zone are probably within several tenths of a degree of reality.

[15] In Figure 5 we compare plots of modeled and observed SAT for representative long-running, reliable meteorological station locations, 04250 and 04360, on the west and east sides of southern Greenland. These locations are relatively low latitude and are expected to be near relatively high melt/runoff regions of the GrIS margin. Striking agreements of modeled with observed SAT values and variability are apparent. A problem is that the DMI SAT data are not really independent as they were assimilated into the scheme used to produce the ECMWF (re)analyses, but the comparison nevertheless demonstrates significantly improved modeled SAT once ECMWF orography errors have been allowed for. Fortunately, the GC-Net SAT observations were not assimilated into the ECMWF analyses, so they are fully independent; a comparison of modeled versus observed SAT for the Swiss Camp meteorological research tower again shows excellent agreement (Figure 6). These are some of the longest-running and most reliable SAT data available for interior Greenland. Swiss Camp is near the western margin of the ice sheet and at relatively low elevation (1169 m), so it lies well within the runoff zone. The results of these comparisons help justify running our

Table 2. Differences Between Corrected ECMWF-Based and in Situ Surface Air Temperatures, Based on All Available Monthly Mean Data for 1958–2003[a]

Station	Surface Air Temperature Difference, K
DMI 04202	−1.5
04210	−0.0
04220	−0.3
04221	−2.5
04230	0.4
04231	1.7
04250	0.9
04260	−0.1
04270	−3.1
04272	−0.2
04310/12	0.1
04320	−0.4
04330	0.3
04339	−1.0
04351	1.2
04360	0.2
04382	2.3
04390	1.7
DMI mean	−0.02
GC-Net Swiss Camp	0.5
Crawford Point 1	2.2
NASA-U	2.3
GITS	1.6
Humboldt	2.9
Summit	1.4
Tunu-N	3.1
DYE-2	2.8
JAR 1	0.5
Saddle	1.9
South Dome	−0.4
NASA-E	2.5
Crawford Point 2	2.0
NGRIP	1.6
NASA-SE	−0.9
KAR	0.5
JAR2	0.5
KULU	−1.0
JAR3	−0.5
Aurora	2.2
GC-Net mean	1.3

[a]Positive bias means ECMWF has higher value.

degree-day meltwater runoff model with (corrected) ECMWF data.

3. Runoff Models

3.1. Theoretical Basis

[16] Our monthly runoff/retention model has been adapted from the annual runoff/retention degree-day model (DDM) of *Janssens and Huybrechts* [2000]. This model uses the integrated sum of expected positive degree days, based on a sinusoidal yearly march of temperature, and different degree-day factors (DDFs) for snow and ice to calculate surface melt and subsequent runoff. Runoff is assumed to occur when melt exceeds a certain fraction of P; hence SAT and P are the important inputs to this type of model. The DDM has the advantage over a more complex energy balance model (EBM) in that it requires relatively few and simpler input data. Surface energy balance and heat flux data required by data hungry EBMs are far more difficult to apply and validate over large areas such as an ice sheet. Also it is hard to parameterize spatial and temporal variations in albedo and roughness. Several studies have shown a close relation between SAT and melt rates [e.g., *Braithwaite*, 1995]. Although DDFs suffer from constraint when derived one place and applied elsewhere, DDFs used here are typical of Greenland sites in the summer ablation zone [*Braithwaite*, 1995]. DDM results can easily be iterated during repeat model runs to correct for initial errors in surface orography and SAT or to downscale model results for example to a higher-resolution orography (section 2).

[17] The new monthly runoff model uses downscaled/corrected SAT and P-E from ECMWF analyses to calculate a rain fraction and subsequently the melt on a month-by-month basis. The rain fraction was calculated as proportional to the time fraction with SAT >1°C [*Janssens and Huybrechts*, 2000]. Any liquid water initially refreezes if the snowpack is cold enough, then it fills the pores until the saturated snow density is reached, and after that stage, runoff occurs, removing saturated snow (snow plus capillary water). When the snow has gone, ice melt can take place. Our runoff model incorporates the *Pfeffer et al.* [1991] retention scheme, which is based on a simple thermodynamic parameterization of the refreezing process [*Janssens and Huybrechts*, 2000]. Heat required for refreezing is set proportional to the heat required to warm the uppermost, thermally active layer, nominally taken to be 2 m, to the melting point. The temperature of this layer T is set equal to the mean annual temperature for $T < 0°C$; otherwise $T = 0°C$. The code handles all zones on the ice sheet, and for a narrow zone above the equilibrium line it also refreezes any meltwater retained in the snowpack at the end of the ablation season to produce superimposed ice. We have run the monthly code in parallel with the annual code [*Janssens and Huybrechts*, 2000], which works similarly except for time resolution, and we evaluate and present results from both models below.

[18] Theoretically, the monthly runoff model should give more reliable/accurate results because it simulates a more "interactive" atmosphere/surface. The main difference of the monthly code as compared to the annual code is the monthly resolution of the P-E input, whereas in the annual code P is assumed to be available in its entirety at the beginning of the melt season. However, note that both models evaluate the melt monthly. As a consequence, in some cases the monthly code may produce ice melt earlier than in the annual code as the snowpack in a particular summer month has already disappeared before reappearing later, whereas the annual code would lump all snow accumulation together before the melting starts. This aspect will be studied below (section 4.2). As the monthly code tracks mass and elevation changes on a month by month basis, allowing for a fluent transition between balance years, it is (in theory) best suited to be forced with a continuous time series as is done in this paper.

3.2. Control Model Run

[19] Using their SAT parameterization and P field thought to be representative of the second half of the twentieth century (C20th), *Janssens and Huybrechts* [2000] obtained a GrIS runoff of ~280 $km^3\ yr^{-1}$. (Note that this and all other subsequent values referred to are in water equivalent, WE.) For comparison, the mean GrIS runoff of eight models cited by *Church et al.* [2001] is 297 ± 32 $km^3\ yr^{-1}$. These

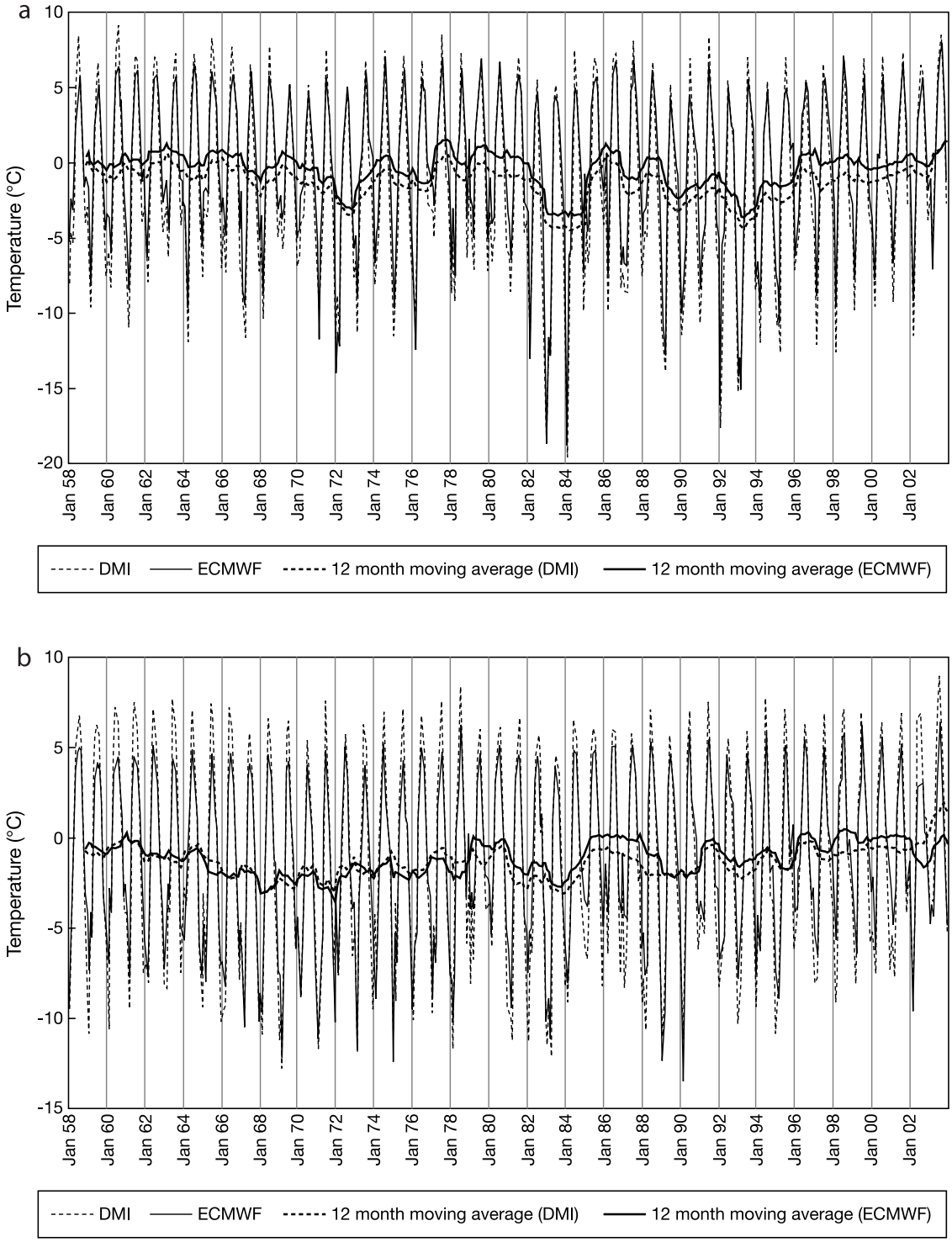

Figure 5. (a) Modeled (ECMWF) and observed (DMI) 2-m temperature at 04250. (b) Modeled (ECMWF) and observed (DMI) 2-m temperature at 04360. Note the sign change of 12-month running mean between reanalysis and forecast model.

values are for the conterminous ice sheet and attached ice shelves but exclude small ice caps and disconnected glaciers. The SAT parameterization of *Janssens and Huybrechts* [2000] comes from a data set of Greenland temperatures used by *Reeh* [1991], and was first published by *Huybrechts et al.* [1991]. *Janssens and Huybrechts* [2000] P data set is based on precipitation data of *Ohmura and Reeh* [1991], updated using shallow ice core data from more recent traverses in north Greenland [*Jung-Rothenhäusler*, 1998]. The total annual P used by *Janssens and Huybrechts* [2000] was $\sim$542 km^3 yr^{-1} (= 0.321 m yr^{-1} of water depth averaged across the ice sheet). The latter

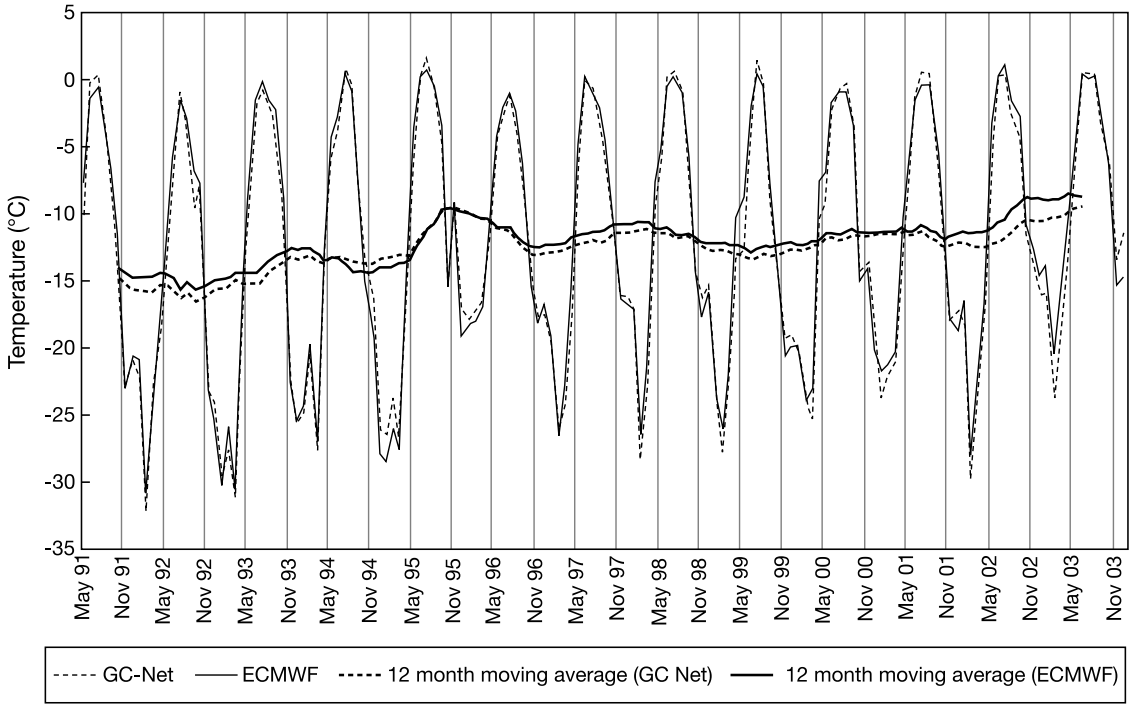

Figure 6. Modeled (ECMWF) and observed 2-m temperature at Swiss Camp.

value is similar to our recent assessment of 1961–1990 mean annual P-E (0.335 m yr^{-1}) based on ERA-40 reanalysis data, backed up by verification with the latest NASA Program in Arctic Regional Climate Assessment (PARCA) ice cores [*Hanna et al.*, 2005].

[20] Our control model run, against which we compare our ECMWF-based runoff results (section 4), is the annual runoff model run with the *Janssens and Huybrechts* [2000] SAT and P treatments and, like Janssens and Huybrechts, including area factors for map projection distortions. This gives 268 km^3 yr^{-1} runoff for the conterminous ice sheet and 279 km^3 yr^{-1} if ice shelves are included. These are the same values as given by *Janssens and Huybrechts* [2000]. Ice shelves add only 0.25% to the GrIS area ($\sim 1.69 \times 10^6$ km^2), but they add a disproportionate amount ($\sim$4%) of runoff because they are low lying (almost at sea level) and therefore relatively warm in summer. However, as the ice shelves are not relevant for sea level change estimates based on SMB variations, we do not include them here except in one case to be mentioned later (see section 6). The spatial distribution of runoff from our model control run (without ice shelves) is shown in Figure 7. This shows the greatest runoff in SW Greenland, around and just south of Jakobshavn Isbrae. Here marginal values exceeding 5 m yr^{-1} runoff are typical. Elevation slopes are generally gentler in SW than SE Greenland; comparison of Figures 7 and 1 shows that elevation, through its relation with lapse rates and SAT, has a strong control on runoff.

4. Greenland Ice Sheet Runoff Series

4.1. Annual Model

[21] We ran the annual model using monthly SAT and annual P-E data from the (re)analysis. GrIS runoff and SMB thus derived for the whole analysis period (1958–2003) and various intermediate periods are shown in Table 3. We consider 1961–1990 because it is equivalent to a major climatological standard "normal" period (e.g., for comparison with Greenland station normals presented by *Cappelen et al.* [2001]). The 1961–1990 period also represents later C20th averages, which are largely independent of the recent

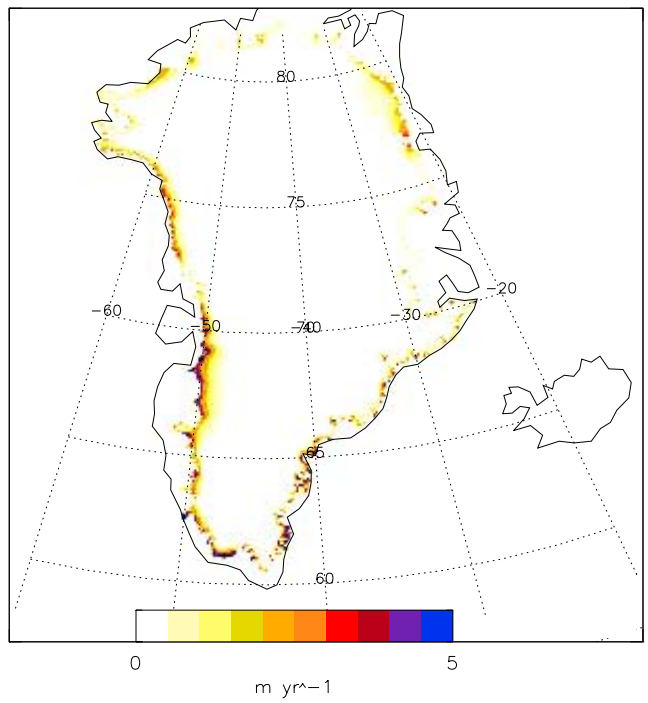

Figure 7. Greenland ice sheet runoff from control model run.

Table 3. Greenland Ice Sheet (Excludes Ice Shelves) Mean Annual Precipitation Minus Evaporation, Runoff, and Surface Mass Balance for Various Periods, as Modeled Using ECMWF (re)Analysis Data and the *Janssens and Huybrechts* [2000] Runoff/Retention Model[a]

Period	P-E	Runoff	SMB
1958–2003	573 (σ = 70)	280 (σ = 69)	293 (σ = 104)
1961–1990	562	264	298
1993–1998	586	324	262
1998–2003	614	372	241

[a]Values are km^3 yr^{-1} water equivalent. Standard deviations (σ) are given for the full 1958–2003 period.

comprehensive measuring program [e.g., *Krabill et al.*, 2004; *Thomas and PARCA Investigators*, 2001] or of any recent temperature rises/mass balance effects that might have been caused by global warming [*Intergovernmental Panel on Climate Change*, 2001]. Other intermediate periods examined are 1993–1998 (coincident with the *Krabill et al.* [2000] airborne laser surveys of the GrIS) and 1998–2003, the latter to try to gauge any very recent changes in runoff that might have occurred.

[22] ECMWF-based mean annual runoff (MAR) for 1961–1990 is 264 km^3 yr^{-1} (WE ice sheet volume excluding ice shelves, allowing for areal distortions), which is only ~2% below the *Janssens and Huybrechts* [2000] value (270 km^3 yr^{-1} excluding ice shelves) for later C20th runoff (Table 3). This indicates that the SAT and P treatments used by *Janssens and Huybrechts* [2000] are very similar to the 1961–1990 climatological mean, which is more or less as expected as the SAT parameterization is based on 10-m subsurface firn temperatures and the P field was homogenized for the second half of the C20th by *Ohmura and Reeh* [1991]. The good agreement between our 1961–1990 runoff and our control model (3.1) runoff helps justify feeding the runoff models with ECMWF reanalysis data.

[23] We show a map of differences between 1961–1990 MAR from the annual runoff model/ECMWF data and annual runoff from the model control run referenced above (Figure 8). Although both simulations capture similar amounts of runoff for the whole GrIS, values are considerably (up to ~2 m yr^{-1} WE ice sheet averaged depth) higher on the basis of ECMWF in inland southwest Greenland ~67°N near 04231 Kangerlussuaq, in W Greenland between 72.5°N and 76.5°N, around much of the north Greenland margin, and in E Greenland from ~70° to 75°N. ECMWF-based runoff was up to ~2 m yr^{-1} less than the model control run in other areas. Spatial differences may reflect remaining biases in either our corrected SAT from ECMWF (there is apparent partial agreement with modeled-observed SAT differences shown in Table 2) and/or in the *Janssens and Huybrechts* [2000] SAT parameterization.

[24] The full 1958–2003 annual model runoff series is shown in Figure 9. The least squares linear regression trend line increase for the whole period was +101 km^3 yr^{-1}, considerably greater than the standard deviation (σ) of 69 km^3 yr^{-1} and therefore a statistically significant overall increase. Subdividing the period reveals a nonsignificant trend line increase of runoff of +46 km^3 yr^{-1} for 1958–1990, <1σ (55 km^3 yr^{-1}) for those years. MAR steadily increased during the 1990s to reach 372 km^3 yr^{-1} in 1998–2003: This is also >1σ above the 1961–1990 MAR, so it can be regarded as significantly higher (Table 3). So most of the rise in runoff came late in the record and corresponds with increased coastal thinning measured around the GrIS margins by repeat airborne laser surveys over the past few years [*Krabill et al.*, 2004]. Greatest increases in (1961–1990) to (1998–2003) MAR were in much of west, SW, and extreme NW Greenland, with relatively little change, or even a decrease in runoff, in the SE (Figure 10). This may reflect different climatic regimes, hence recent atmospheric circulation and SAT changes, on opposite sides of Greenland [*Cappelen et al.*, 2001]. However, during the same period, mean annual P-E also rose by a statistically insignificant amount from 562 km^3 yr^{-1} in 1961–1990 to 614 km^3 yr^{-1} in 1998–2003, partly offsetting increased runoff. So although mean annual SMB decreased from 298 km^3 yr^{-1} in 1961–1990 to 241 km^3 yr^{-1} in 1998–2003, this decrease was insignificant given the much larger SD in SMB of 104 km^3 yr^{-1}.

4.2. Monthly Models

[25] The monthly model M1 was run with monthly SAT and P-E forcing based on ECMWF analyses and surprisingly yields a much higher 1961–1990 mean annual runoff of 390 km^3 yr^{-1} for the GrIS. This is much (~48%) greater than MAR for the same period from the annual model. The difference is due to precipitation forcing, as both the annual and monthly codes were forced using the same direct monthly temperature data input. Model M1 runs out of snow during the summer and so ice melt takes place earlier than in the annual model. There are at least two possible reasons why this might be the case. One is the seasonal variation in precipitation, which is most evident in southern

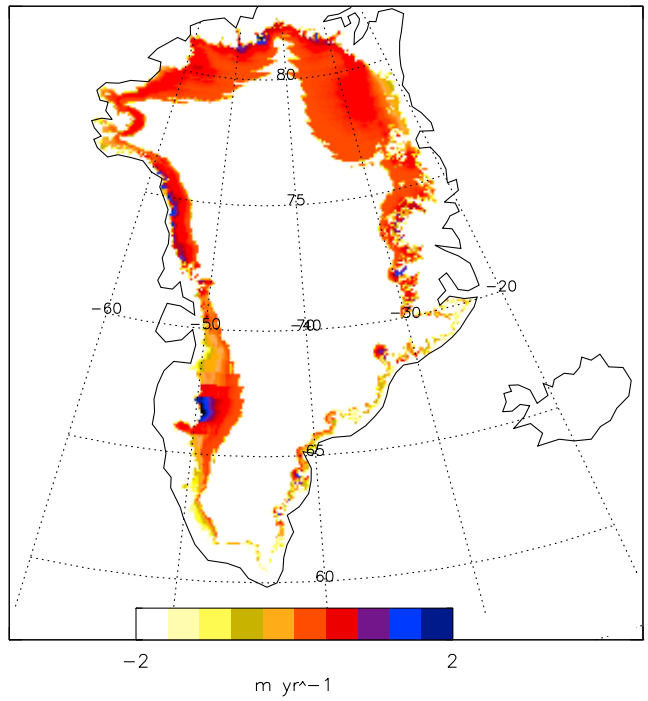

Figure 8. GrIS 1961–1990 mean annual runoff minus control model run runoff.

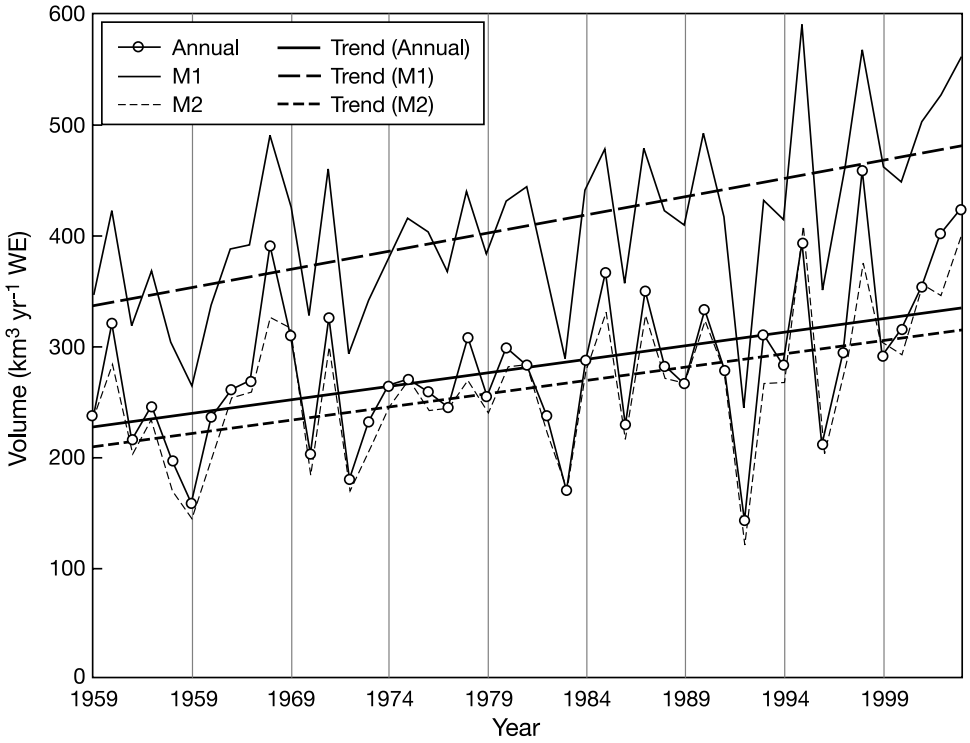

Figure 9. Greenland ice sheet meltwater runoff loss from annual and monthly (M1 using P-E and M2 P only) degree-day runoff/retention models.

Greenland: In the southeast, where most precipitation falls, Greenland summers are generally drier than Greenland winters; for example, at 04360 Tasiilaq, 1961–1990 mean monthly precipitation is 120 mm in January and 47 mm in July [*Cappelen et al.*, 2001]. The second is that modeled evaporation (from SLHF) is probably too high in some marginal areas in summer (>0.5 m yr^{-1} for July), compared with an existing sublimation climatology from GC-Net station data [*Box and Steffen*, 2001], artificially depressing P-E is below its "real" value during the key summer months. This does not seem to matter much for the annual model because just the gross annual values of P and E are used, so that the hypothesized surplus of E for 1 or 2 months has a much lower impact on calculated runoff.

[26] Therefore, using another version of the monthly model, M2, we used P instead of P-E as input; in all other aspects the M1 and M2 model runs were identical. The resulting MAR derived using M2 is 247 km^3 yr^{-1} for 1961–1990. The 1961–1990 MAR obtained using the equivalent form A2 (using P instead of P-E) of the annual model is almost the same (244 km^3 yr^{-1}). These values are 94% and 93%, respectively, of that from the standard annual model (using P-E). This is unsurprising: If we don't include evaporation in our runoff model, there is probably too much input water, which means that the threshold required for runoff to occur is now somewhat higher than should be the case; hence modeled runoff is lower. Comparative runoff series from the annual and two monthly models (M1 using P-E and M2 using P only) are shown in Figure 9.

[27] We first considered scaling up the M2 model estimates by ~6.5% so that the 1961–1990 MAR is then equivalent to that from the annual model. This is justifiable on the basis of very strong correlations between annual (1959–2003) runoff series of the (1) annual and (2) unscaled monthly runoff models, both M1 and M2 (r = 0.97), and annual runoff series of the unscaled monthly runoff models M1 and M2 (r = 0.98).

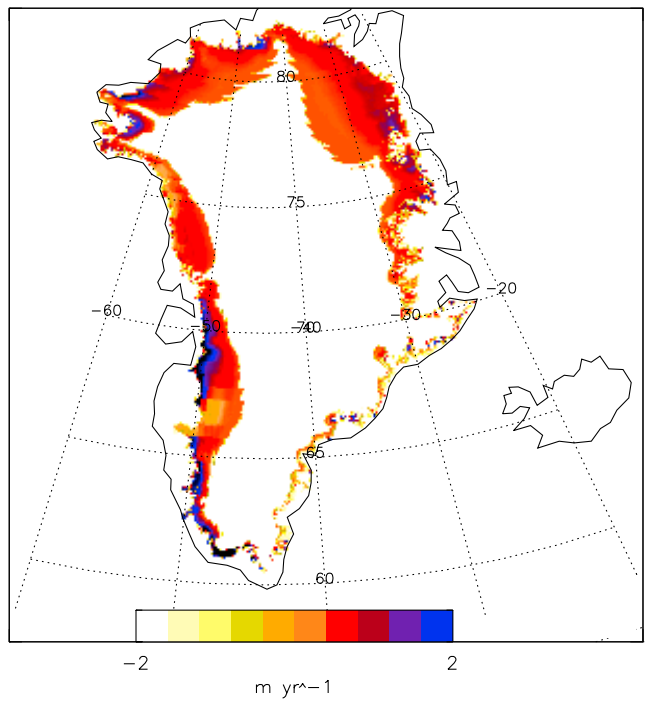

Figure 10. GrIS (2002–2003) to (1961–1990) mean annual runoff from annual runoff model.

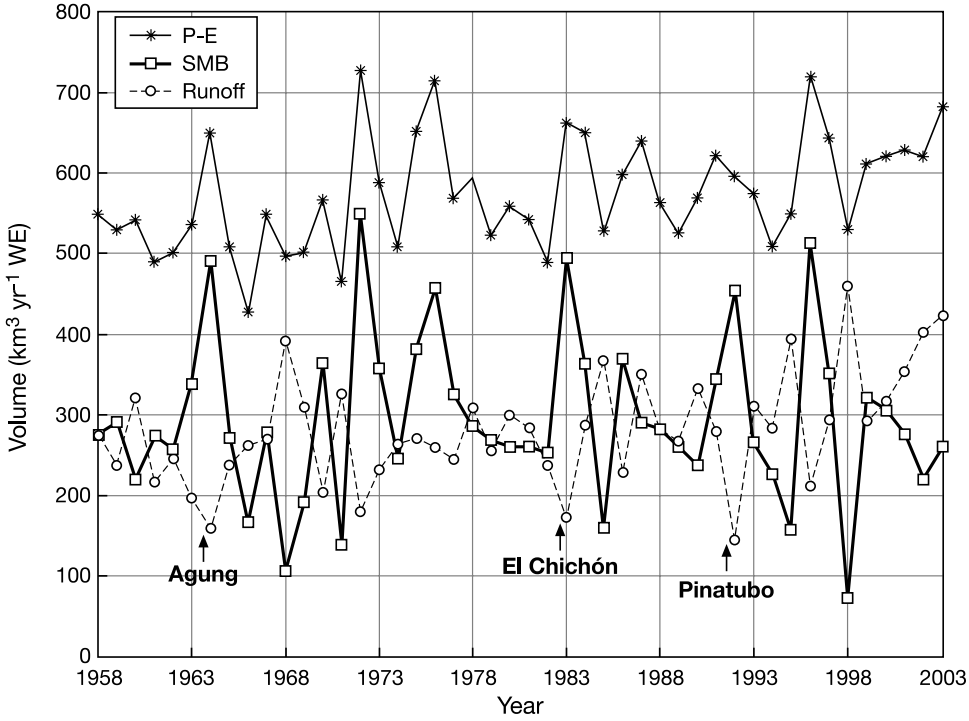

Figure 11. Greenland ice sheet surface mass balance series for past 46 years.

[28] Our scaled-up annual runoff series derived using M2 is very similar to the annual model series. We ultimately elected to use the annual runoff model results, as these did not require any scaling and are sufficient for our current purposes. We refer to the annual model estimates in the remainder of this paper.

5. Greenland Ice Sheet Surface Mass Balance History and Links With Climate

[29] We present for the first time in the published literature a Greenland ice sheet surface mass balance series (including P-E and runoff) for the past 46 years (1958–2003) (Figure 11). This shows considerable variability in all three series, SD about 70 $km^3\ yr^{-1}$ WE (12% of mean annual value) in P-E, 69 $km^3\ yr^{-1}$ WE (25% of mean) in runoff, and 104 $km^3\ yr^{-1}$ WE in SMB, but it also well depicts the general rising trend in runoff since the early 1990s.

[30] It is important to bear in mind that individual yearly values in the following discussion are of modeled P-E and runoff and have respective estimated standard errors of ~5% and ~10%. The former is from a comparison of modeled P-E with ice core data [*Hanna et al.*, 2005]; the latter is from our remaining mean SAT error less than ~0.5 K. This assessment of our remaining model errors is approximately the same order of magnitude as the standard deviation of the accumulation and runoff values listed by *Church et al.* [2001]. The associated inherent uncertainty in modeled SMB naturally comes from combining these standard errors (SEs) and equals the square root of the sum of squares of the SEs of P-E and runoff. This means the greater the values of runoff and P-E, the more uncertainty there is in derived SMB, a possibly salient point given the recent significant increase in runoff.

[31] The year with greatest modeled runoff is 1998 (457 $km^3\ yr^{-1}$), and two other years have >400 $km^3\ yr^{-1}$ (421 $km^3\ yr^{-1}$ in 2003 and 401 $km^3\ yr^{-1}$ in 2002); next is 1995 (393 $km^3\ yr^{-1}$) (Table 4). Significantly, all five highest-runoff years are within the past decade, and they include the previously established peaks of 1995 and 1998 [*Hanna et al.*, 2002] as well as two of the three most recent melt seasons. The recent increase in GrIS runoff, and record runoff years, may be associated with a recent strong warming in southern Greenland which began in the early 1990s [*Hanna and Cappelen*, 2003]. Our significant increasing runoff trend 1958–2003 is apparently paradoxical given the significant −1.29 K 1958–2001 trend line cooling reported by *Hanna and Cappelen* [2003]. However, this overall

Table 4. Five Highest and Five Lowest Runoff and SMB Years (Water Equivalent Ice Sheet Volume)

Runoff, $km^3\ yr^{-1}$	Year	SMB, $km^3\ yr^{-1}$	Year
456.5[a]	1998	547.6[a]	1972
421.0	2003	510.2	1996
400.5	2002	492.7	1983
392.7	1995	490.7	1964
390.8	1968	455.5	1976
197.1[b]	1963	158.0[b]	1985
178.9	1972	155.3	1995
169.2	1983	137.7	1971
158.2	1964	104.9	1968
142.1	1992	71.0	1998

[a]Highest runoff and SMB year.
[b]Lowest runoff and SMB year.

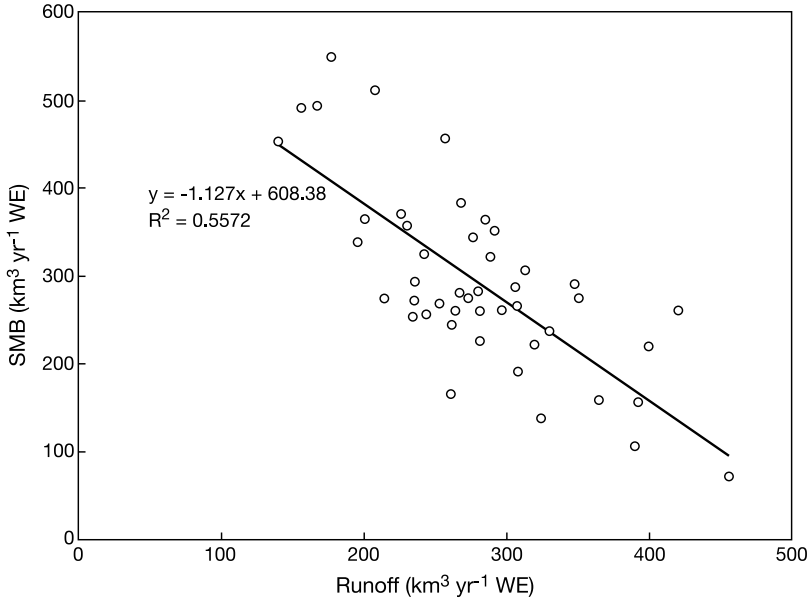

Figure 12. Greenland ice sheet surface mass balance versus runoff.

cooling was concentrated in the colder seasons, and an extended, updated analysis of the Greenland climate data shows an overall but insignificant 1961–2003 least squares linear regression summer warming trend of +0.45 K. Coastal southern Greenland stations significantly warmed in summer by +1.30 K trend line increase 1990–2003 following an insignificant −0.58 K summer cooling trend 1961–1990 [*Cappelen and Hanna*, 2004].

[32] Also significantly, the lowest-runoff year of the entire 46-year series, 1992 (142 km^3 yr^{-1}) (Table 4), immediately followed the Mount Pinatubo volcanic eruption of 1991, confirming the effect of global dust veils generated by volcanic activity at low latitudes in cooling polar regions and suppressing ice sheet melt. This effect was first observed using satellite-derived melt extent by *Abdalati and Steffen* [1997], but because their series starts in 1979 we have the advantage of a much longer analyzed time series to make our result more robust. Moreover, three of the next four lowest–modeled runoff years followed the two other globally significant volcanic eruptions of the later C20th [*Lamb*, 1995]: Agung (Bali) in 1963 (1963 and 1964 were the fifth- and second-lowest-runoff years in our series) and El Chichón (Mexico) in 1982 (1983 was the third-lowest-runoff year).

[33] Runoff and SMB are significantly inversely correlated (r = −0.75), so that low-runoff years (such as those following major volcanic eruptions) often coincide with high-SMB years, and vice versa (Figure 12). For example, 1992 with its exceptionally low runoff (following Pinatubo) was the sixth-highest-SMB year, only prevented from having an even more significant SMB by its apparently unexceptional P-E (Figure 11). The fourth- and third-highest-SMB years are 1964 and 1983 (following the other two main volcanic eruptions). The volcanic "signature" is not really evident in the P-E record (the latter reflects changes in atmospheric dynamics and circulation). Indeed, runoff and P-E are very poorly correlated (r = −0.13). However, SMB and P-E are significantly positively correlated (r = 0.75), which is unsurprising as SMB depends almost as much on P-E as on runoff (P-E has values generally greater than runoff but this is compensated by its year-to-year variability being lower). The year 1998 was a semidecadal trough in modeled P-E; this combined with the record high annual runoff yielded the lowest SMB in the entire record in 1998 (Figure 11 and Table 4).

[34] Our modeled runoff and SMB series results tentatively suggest the influence of various climatic forcing factors in affecting mass loss and state of balance of the GrIS. Future work should investigate these influences.

[35] A map of mean annual SMB demonstrates high negative values (less than −5 m yr^{-1}) in the lower-lying marginal areas, especially in the west and north, which is simply reflecting the high summer temperatures and runoff in these regions (Figure 13). On the other hand, values are typically +0 to >1 m yr^{-1} SMB across much of the ice sheet interior, with an areal distribution that reflects precipitation and snowfall patterns. It will be interesting to compare SMB changes with surface elevation changes derived from recent airborne laser surveys, to try to assess the degree to which Greenland mass fluctuations, rather than ice flow (dynamics), control elevation changes across the ice sheet. This too will be the subject of a separate study.

6. Overall Mass Balance and Effects on Global Sea Level Rise

[36] We reran the annual runoff model, this time including the ice shelves in our defined GrIS. We derived estimates of GrIS mass balance components, not just SMB but overall mass balance for various periods, by including current best estimates of iceberg calving and bottom melting from ice shelves [*Church et al.*, 2001] (Table 5). Simple combination of standard errors for P-E (5%) and runoff (10%) enabled us to calculate SEs for SMB

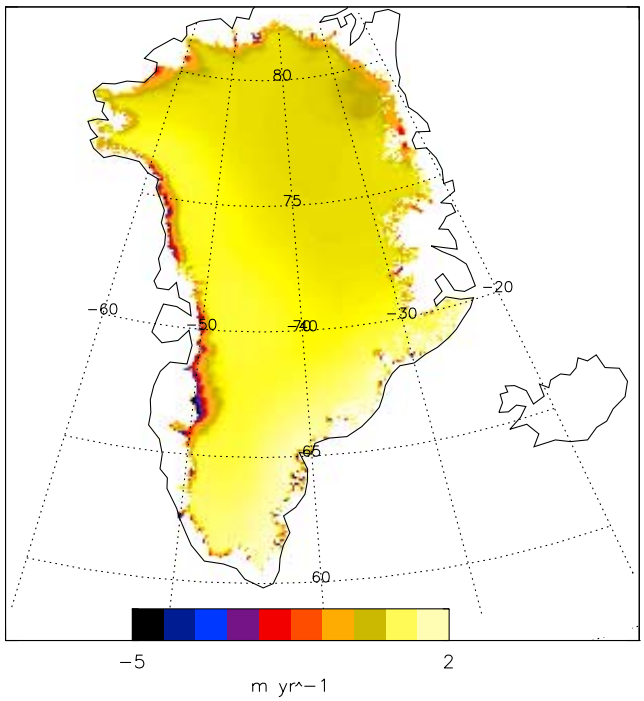

Figure 13. Greenland ice sheet mean annual 1958–2003 surface mass balance.

and, together with standard deviations of iceberg calving and bottom melting estimates given by *Church et al.* [2001], uncertainties for overall mass balance (Table 5). Note that the *Church et al.* [2001] assessment of GrIS mass balance, which can be interpreted as being for the second half of the C20th (climatologically ≅ 1961–1990), has zero within the bounds of the stated error, so it is therefore not significantly different from zero. However, it does suggest a tendency toward a negative mass balance for the GrIS. The *Church et al.* [2001] mass balance is probably too low because it is based on accumulation, which is substantially less than precipitation (a considerable fraction of Greenland precipitation falls as rain), and we have already seen that modeled melt is sensitive to the value we take for annual mass input (less input means more melt). *Janssens and Huybrechts* [2000] derived a mass balance from their annual runoff model that is very close to zero (-5 ± 51 km^3 yr^{-1}), which when combined with the IPCC estimates for iceberg calving and melting below the ice shelves [*Church et al.*, 2001], can again be interpreted as being for the 1961–1990 climatological period. The last three columns present best estimates of SMB and mass balance (including ice shelves) from our ECMWF-based runoff model results, and the first of these shows a mass balance for 1961–1990 (22 ± 51 km^3 yr^{-1}) that is not significantly different from the *Janssens and Huybrechts* [2000] value for the equivalent period.

[37] The final two columns in Table 5 show declining SMB and increasingly negative mass balance for 1993–1998 and 1998–2003, although mass balance is not significantly negative even for the later period. However, the "real" mass balance is probably substantially more negative because we do not take into account dynamical factors forcing the ice flow over the decadal timescale, and these are likely to be significant, especially near the ice sheet margins [e.g., *Krabill et al.*, 2004; *Thomas et al.*, 2003; *Zwally et al.*, 2002]. Also, our best estimates of -14 ± 55 km^3 yr^{-1} and -36 ± 59 km^3 yr^{-1} mass balance for 1993–1998 and 1998–2003 are much less than the -59 km^3 yr^{-1} and -80 km^3 yr^{-1} mass losses derived from airborne laser surveys for the same respective periods [*Krabill et al.*, 2004], the latter including dynamical effects. This suggests that ice dynamical effects (enhanced ice sheet flow) may have been the main factor driving the surface lowering widely observed around the GrIS margins during this period. Alternatively, it is possible that our figure is a substantial underestimate of mass lost from the ice sheet during this period because we do not account for possibly enhanced iceberg calving and/or bottom melting during the most recent years (since about 1990) but merely use the current best available estimates for these parameters reported by *Church et al.* [2001].

[38] Alternatively, we can consider the ((1961–1990) to (1998–2003)) decrease in our modeled mass balance, which is similar whether or not we include the ice shelves' area in our calculations (58 km^3 yr^{-1} and 57 km^3 yr^{-1}, respectively). With effectively zero mass balance estimates given by *Church et al.* [2001] and *Janssens and Huybrechts* [2000], we can reasonably assume that the ice sheet was in approximate mass balance and dynamic equilibrium for earlier C20th conditions. This implies a contribution to global sea level rise of the order of 0.15 mm yr^{-1} averaged over the last 6 years, just from changes in SMB. Again, the true figure is probably somewhat larger than this, because of a likely greater ice dynamical effect accompanying the enhanced melting. Of course, the net contribution of Greenland to global sea level rise is likely to become much more significant by 2100 as Greenland SATs rise and more ice

Table 5. Greenland Ice Sheet Mass Balance Components[a]

	Church et al. [2001]	*Janssens and Huybrechts* [2000]	ECMWF 1961–1990	ECMWF 1993–1998	ECMWF 1998–2003
P-E[b]	520 ± 26[c]	542	562	586	614
Runoff[b]	297 ± 32	281	273	334	383
SMB	225 ± 41	262 ± 39	289 ± 39	253 ± 44	231 ± 49
Iceberg calving	235 ± 33				
Bottom melting	32 ± 3				
Mass balance	−44 ± 53	−5 ± 51	22 ± 51	−14 ± 55	−36 ± 59

[a]Ice shelves are included for purpose of comparison with *Church et al.* [2001] estimates of mass balance. Values are km^3 yr^{-1} water equivalent. Combination of standard errors gives estimated overall errors in SMB and mass balance.
[b]Estimated 5% uncertainty for P-E and 10% uncertainty for runoff in ECMWF-based estimates.
[c]Accumulation. P-E will be greater because it includes rainfall as well as snow.

melts. A recent modeling study gives an average C21st number of +0.47 mm yr^{-1}, with a predicted range between +0.32 and +0.98 mm yr^{-1} for the last decade of the C21st for all GCM forcings [*Huybrechts et al.*, 2004].

7. Conclusions

[39] We have presented runoff and SMB series for the past 46 years for the Greenland ice sheet. Our runoff model has been validated partly through comparisons of modeled with observed surface air temperature and partly through a control model run. These series yield useful insights into the current state and variability of mass balance of the ice, and so they may help us refine future predictions of the ice. There is a distinct signature of the three main later C20th volcanoes being followed by low-runoff years. Runoff increased significantly over the past decade, looking at the whole record, but, because of a contemporaneous rise in P-E, not enough to significantly change (yet) SMB. On the other hand, there seems likely to have been a reduction in overall mass balance of the ice sheet over the past few decades, with an accompanying positive effect on global sea level rise; our best estimate from SMB changes alone is +0.15 mm yr^{-1} during 1998–2003, plus a likely additional contribution from ice dynamics. The recent mass loss may become much more significant during the next few decades. Next steps are to explore various applications of this new glaciological data set tool, in particular links with climatic forcing factors, to try to assess the degree of interaction between Greenland ice and climate.

[40] **Acknowledgments.** We thank the British Atmospheric Data Centre and ECMWF for providing (re)analysis data; Grant Bigg, Roger Braithwaite, Alan Condron, Tris Irvine-Fynn, Tim Osborn, Peter Smithson, and Pedro Viterbo for advice; and Paul Coles for drawing Figure 1. Two anonymous reviewers made valuable suggestions that helped improve the paper. Support for P. Huybrechts and I. Janssens came from the Belgium Science Policy Office Second Programme on Global Change and Sustainable Development project MILMO (contract EV/10/9B).

References

Abdalati, W., and K. Steffen (1997), The apparent effects of the Mt. Pinatubo eruption on the Greenland ice sheet melt extent, *Geophys. Res. Lett.*, *24*, 1795–1797.

Abdalati, W., and K. Steffen (2001), Greenland ice sheet melt extent: 1979–1999, *J. Geophys. Res.*, *106*, 33,983–33,988.

Box, J. E., and K. Steffen (2001), Sublimation on the Greenland ice sheet from automated weather station observations, *J. Geophys. Res.*, *106*, 33,965–33,981.

Box, J. E., D. H. Bromwich, and L.-S. Bai (2004), Greenland ice sheet surface mass balance for 1991–2000: Application of Polar MM5 mesoscale model and in situ data, *J. Geophys. Res.*, *109*, D16105, doi:10.1029/2003JD004451.

Braithwaite, R. J. (1995), Positive degree-day factors for ablation on the Greenland ice sheet studied by energy-balance modeling, *J. Glaciol.*, *41*, 153–160.

Braithwaite, R. J., and O. B. Olesen (1993), Seasonal variation of ice ablation at the margin of the Greenland ice sheet and its sensitivity to climate change, Qamanarssup sermia, West Greenland, *J. Glaciol.*, *39*, 267–274.

Braithwaite, R. J., O. B. Olesen, and H. H. Thomsen (1992), Calculated variations of annual ice ablation at the margin of the Greenland ice sheet, West Greenland, 1961–90, *J. Glaciol.*, *38*, 266–272.

Cappelen, J., and E. Hanna (2004), Overall cooling in coastal southern Greenland over the past 45 years and relation with the North Atlantic Oscillation, paper presented at 5th European Conference on Applied Climatology, Eur. Clim. Support Network, Nice, France, 28 Sept.

Cappelen, J., B. V. Jørgensen, E. V. Laursen, L. S. Stannius, and R. S. Thomsen (2001), The observed climate of Greenland, 1958–99 with climatological standard normals, 1961–90, *Tech. Rep. 00-18*, Danish Meteorol. Inst. Minist. of Transp., Copenhagen.

Church, J. A., J. M. Gregory, P. Huybrechts, M. Kuhn, C. Lambeck, M. T. Nhuan, D. Qin, and P. L. Woodworth (2001), Changes in sea level, in *Climate Change 2001: The Scientific Basis—Contribution of Working Group I to the Third Assessment Report of the Intergovernmental Panel on Climate Change*, edited by J. T. Houghton et al., pp. 639–694, Cambridge Univ. Press, New York.

Ekholm, S. (1996), A full coverage, high-resolution, topographic model of Greenland computed from a variety of digital elevation data, *J. Geophys. Res.*, *101*, 21,961–21,972.

Gregory, J. M., P. Huybrechts, and S. Raper (2004), Threatened loss of the Greenland ice sheet, *Nature*, *428*, 616, doi:10.1038/428616a.

Hanna, E., and J. Cappelen (2003), Recent cooling in coastal southern Greenland and relation with the North Atlantic Oscillation, *Geophys. Res. Lett.*, *30*(3), 1132, doi:10.1029/2002GL015797.

Hanna, E., and P. Valdes (2001), Validation of ECMWF (re)analysis surface climate data, 1979–1988, for Greenland and implications for mass balance modelling of the Ice Sheet, *Int. J. Climatol.*, *21*, 171–195.

Hanna, E., P. Valdes, and J. McConnell (2001), Patterns and variations of snow accumulation over Greenland, 1979–98, from ECMWF analyses and their verification, *J. Clim.*, *14*, 3521–3535.

Hanna, E., P. Huybrechts, and T. Mote (2002), Surface mass balance of the Greenland ice sheet from climate-analysis data and accumulation/runoff models, *Ann. Glaciol.*, *35*, 67–72.

Hanna, E., J. McConnell, S. Das, J. Cappelen, and A. Stephens (2005), Observed and modeled Greenland ice sheet snow accumulation, 1958–2003, and links with regional climate forcing, *J. Clim.*, in press.

Huybrechts, P., and J. de Wolde (1999), The dynamic response of the Greenland and Antarctic ice sheets to multiple-century climatic warming, *J. Clim.*, *12*, 2169–2188, doi:10.1175/1520-0442(1999)012.

Huybrechts, P., A. Letréguilly, and N. Reeh (1991), The Greenland ice sheet and greenhouse warming, *Global Planet. Change*, *3*, 399–412.

Huybrechts, P., J. Gregory, I. Janssens, and M. Wild (2004), Modelling Antarctic and Greenland volume changes during the 20th and 21st centuries forced by GCM time slice integrations, *Global Planet. Change*, *42*, 83–105, doi:10.1016/j.gloplacha.2003.11.011.

Intergovernmental Panel on Climate Change (2001), *Climate Change 2001: The Scientific Basis—Contribution of Working Group I to the Third Assessment Report of the Intergovernmental Panel on Climate Change*, Cambridge Univ. Press, New York. (Available at http://www.grida.no/climate/ipcc_tar/wg1/index.htm)

Janssens, I., and P. Huybrechts (2000), The treatment of meltwater retention in mass-balance parameterizations of the Greenland ice sheet, *Ann. Glaciol.*, *31*, 133–140.

Jung-Rothenhäusler, F. (1998), Remote sensing and GIS studies in North-East Greenland Bremerhaven, *Ber. Polarforschung*, *280*, 161 pp.

Krabill, W., W. Abdalati, E. Frederick, S. Manizade, C. Martin, J. Sonntag, R. Swift, R. Thomas, W. Wright, and J. Yungel (2000), Greenland ice sheet: High-elevation balance and peripheral thinning, *Science*, *289*, 428–430.

Krabill, W., et al. (2004), Greenland ice sheet: Increased coastal thinning, *Geophys. Res. Lett.*, *31*, L24402, doi:10.1029/2004GL021533.

Lamb, H. H. (1995), *Climate, History and the Modern World*, 2nd ed., Routledge, Boca Raton, Fla.

Mote, T. L. (2003), Estimation of runoff rates, mass balance, and elevation changes on the Greenland ice sheet from passive microwave observations, *J. Geophys. Res.*, *108*(D2), 4056, doi:10.1029/2001JD002032.

Oerlemans, J. (1991), The mass balance of the Greenland ice sheet: Sensitivity to climate change as revealed by energy-balance modelling, *Holocene*, *1*, 40–49.

Ohmura, A., and N. Reeh (1991), New precipitation and accumulation maps for Greenland, *J. Glaciol.*, *37*, 140–148.

Ohmura, A., M. Wild, and L. Bengtsson (1996), A possible change in mass balance of Greenland and Antarctic ice sheets in the coming century, *J. Clim.*, *9*, 2124–2135.

Pfeffer, W. T., M. F. Meier, and T. H. Illangasekare (1991), Retention of Greenland runoff by refreezing: Implications for projected future sea level change, *J. Geophys. Res.*, *96*, 22,117–22,124.

Reeh, N. (1991), Parameterisation of melt rate and surface temperature on the Greenland Ice Sheet, *Polarforschung*, *59*, 113–128.

Simmons, A. J., and J. K. Gibson (2000), The ERA-40 project plan, *ERA-40 Proj. Rep. 1*, Eur. Cent. for Med.-Range Weather Forecasts, Reading, U. K.

Steffen, K., and J. E. Box (2001), Surface climatology of the Greenland ice sheet: Greenland climate network 1995–1999, *J. Geophys. Res.*, *106*, 33,951–33,964.

Thomas, R. H., and PARCA Investigators (2001), Program for Arctic Regional Climate Assessment (PARCA): Goals, key findings, and future directions, *J. Geophys. Res.*, *106*, 33,691–33,705.

Thomas, R. H., et al. (2003), Investigation of surface melting and dynamic thinning on Jakobshavn Isbrae, Greenland, *J. Glaciol.*, *49*, 231–239.

Zwally, H. J., et al. (2002), Surface melt-induced acceleration of Greenland ice-sheet flow, *Science*, *297*, 218–222.

J. Cappelen, Danish Meteorological Institute, Copenhagen DK-2100, Denmark.

E. Hanna, Department of Geography, University of Sheffield, Sheffield S10 2TN, UK. (ehanna@sheffield.ac.uk)

P. Huybrechts, Alfred Wegener Institute, Bremerhaven D-27515, Germany.

I. Janssens, Departement Geografie, Vrije Universiteit, Brussels B-1050, Belgium.

K. Steffen, Cooperative Institute for Research in Environmental Sciences, University of Colorado, Boulder, CO 80309-0216, USA.

A. Stephens, British Atmospheric Data Centre, Rutherford Appleton Laboratory, Chilton OX11 0QX, UK.